

# Wave-particle interactions with parallel whistler waves: nonlinear and time-dependent effects revealed by Particle-in-Cell simulations

Enrico Camporeale<sup>1</sup>, Gaetano Zimbardo<sup>2</sup>

**Abstract.** We present self-consistent Particle-in-Cell simulations of the resonant interactions between anisotropic energetic electrons and a population of whistler waves, with parameters relevant to the Earth's radiation belt. By tracking PIC particles, and comparing with test-particles simulations we emphasize the importance of including nonlinear effects and time evolution in the modeling of wave-particle interactions, which are excluded in the resonant limit of quasi-linear theory routinely used in radiation belt studies. In particular we show that pitch angle diffusion is enhanced during the linear growth phase, and it rapidly saturates. We discuss how the saturation is related to the fact that the domain in which the particles' pitch angle diffuse is bounded, and to the well-known problem of 90° diffusion barrier.

## 1. Introduction

Resonant wave-particle interactions represent one of the most important mechanism that regulate the scattering and loss of energetic particles in the radiation belts [Thorne, 2010]. Among the different waves that can be generated and propagate in the Earth's radiation belt, much attention has been devoted to whistler waves. They are right-handed polarized electromagnetic waves with frequencies ranging between the ion and electron gyrofrequency. Whistler waves are associated with so-called chorus modes that usually present two characteristic frequency bands with a gap in between. An interpretation of such a gap based on linear theory has recently been presented in [Fu *et al.*, 2014]. Whistler waves can be generated by a kinetic instability driven by a temperature anisotropy (with the temperature in the perpendicular direction greater than in the parallel direction). For instance, equatorial whistler-mode chorus can be excited by cyclotron resonance with anisotropic 10-100 KeV electrons injected from the plasmasphere [Summers *et al.*, 2007; Jordanova *et al.*, 2010]. The generation and propagation of whistler-mode chorus in the Earth's radiation belt has been intensively studied: simulations of rising tones have been performed in Katoh and Omura [2007a, b]; Hikishima *et al.* [2009] for loss-cone distributions and in Tao [2014] for bi-Maxwellian; the non-linear wave growth mechanism has been studied, e.g., in Omura *et al.* [2008]; Summers *et al.* [2012]; Omura *et al.* [2012].

The current paradigm for modeling wave-particle interactions in the radiation belt is based on kinetic quasi-linear theory. It means that the particle distribution function follows a diffusive scattering in the adiabatic invariants space, assuming a broadband wave spectrum and low amplitude fluctuations [Kennel and Engelmann, 1966; Jokipii, 1966; Lyons and Thorne, 1973]. Although quasi-linear theory was primarily developed to study the saturation of a linear instability, due to the distribution function diffusion in phase space, and the formation of a plateau, it is customary to employ the so-called 'resonant limit' in radiation belt simulations, that is the limit in which the linear

growth rate tends to zero, and the distribution reaches a marginally stable state [e.g., Summers *et al.*, 1998]. The underlying assumption of such approach is that diffusion due to a quasi-stationary wave spectrum (and the associated longer timescale) is more relevant than the short-lived diffusion occurring during the linear phase of the instability. Alternatively, one can justify the use of the resonant limit by assuming that the diffusing particles are unrelated to the wave, in the sense that they do not belong to the part of the distribution function that is responsible for the development of the kinetic instability. It is important to remind that the calculation of the diffusion coefficients usually incorporate the interactions between waves and resonant particles only, assuming a stationary wave spectrum with a given amplitude [Summers, 2005; Glauert and Horne, 2005; Summers *et al.*, 2007]. Not only this is not realistic during the linear growth phase of the instability, but we note that the dominance of resonant over non resonant interactions in a turbulent wave field has been recently questioned by Ragot [2012].

Although the distribution function diffusion proceeds in a three-dimensional space (for instance, in energy, pitch angle, and radial directions), the timescale between energy/pitch angle and radial diffusion is very well separated, and hence in this paper we focus on two-dimensional diffusion only.

When electron pitch angle undergoes a stochastic quasi-linear diffusion, its mean squared displacement  $\langle \Delta\alpha^2 \rangle$  is expected to grow linearly in time. Indeed, for normal diffusion, the quasi-linear diffusion coefficient  $D$  and  $\langle \Delta\alpha^2 \rangle$  are related by the celebrated Einstein relation  $\langle \Delta\alpha^2 \rangle = 2Dt$ . In this regime, Tao *et al.* [2011] have shown that test-particles simulations are an excellent tool to test the validity of quasi-linear diffusion, by simply assessing the Einstein relation, with the pitch angle statistics gathered from the simulation particles.

Diffusion in pitch angle presents a crucial difference with standard diffusion in physical space, which is commonly represented and understood in statistical terms with the concept of random walk. The difference is that the pitch angle coordinate is defined on a bounded domain, that is  $\alpha \in [0^\circ, 180^\circ]$ . It is well known that diffusion on bounded domains produce a mean squared displacement that saturates in time (in the case of homogeneous diffusion coefficient, to a value that is proportional to the domain length), [e.g., Metzler and Klafter, 2000; Bickel, 2007]. Interestingly, such important feature of pitch angle scattering has not been emphasized and analyzed in the radiation belt literature. Of

<sup>1</sup>Center for Mathematics and Computer Science (CWI), 1098 XG, Amsterdam, Netherlands

<sup>2</sup>Department of Physics, University of Calabria, Ponte P. Bucci, Cubo 31C, I-87036 Rende, Italy

course, once the distribution in pitch angle becomes close to a saturated state, the Einstein relation becomes meaningless, because although individual particles continue diffusing, the diffusion coefficient cannot be correctly evaluated by means of the mean squared displacement (which becomes constant in time). An important consideration, in a space weather perspective, is whether such (local) saturation of the pitch angle distribution can occur in a time scale which is much shorter than the bounce period, over which the diffusion equation is usually averaged (in order to reduce the dimensionality of the problem, and simplify the calculation of the diffusion coefficients).

Another important aspect of quasi-linear diffusion that apparently has been overlooked in radiation belt studies is the so-called '90° problem', that, on the other hand, has been the focus of several works in cosmic-ray acceleration context (see, e.g. *Shalchi and Schlickeiser* [2005]; *Tautz et al.* [2008]; *Qin and Shalchi* [2009]). In such context, it has been shown that quasi-linear theory underestimates the diffusion through 90° angle, which represents an effective diffusion barrier in pitch angle space (we do not mean, by barrier, total reflection, but a very small diffusion). Diffusion through 90° is instead sizable for some particles (depending on their energy), and this can be incorporated in a diffusion model when considering second-order and nonlinear effects.

The main goal of this paper is to characterize the pitch angle and energy scattering of a tenuous population of energetic electrons both during the linear growth and the nonlinear saturation phases of a whistler instability, including nonlinear and time-dependent effects. This is achieved by performing Particle-in-Cell (PIC) simulations, that is by generating the instability in a completely self-consistent way, without the need of further assumptions (contrary to quasi-linear theory). The PIC simulations results will be compared with test-particle simulation. Such comparison will emphasize the inadequacy of employing the resonant limit of quasi-linear theory for the case studied. Indeed, by tracking resonant particles (not test-particle), we show that pitch angle scattering is tremendously enhanced during the linear growth phase of the instability. The decrease of anisotropy due to the development of the whistler instability results in a rapid precipitation in the loss-cone, in a measure much larger than predicted by quasi-linear diffusion due to a non-growing wave activity.

The importance of a correct assessment of the particle diffusion stems from the fact that particle lifetime is approximately estimated, in the weak diffusion limit, as the inverse of the diffusion coefficients evaluated at the equatorial loss-cone angle [*Shprits et al.*, 2007; *Albert and Shprits*, 2009; *Mourenas and Ripoll*, 2012], by assuming that the scattering remains diffusive through multiple bounce periods [*Summers et al.*, 2007]. As a reference number, we note that the bounce period at  $L = 4.5$  for a 1 MeV electron traveling with loss-cone equatorial pitch angle is approximately 0.24 seconds, or  $1.4 \cdot 10^4 \Omega_e^{-1}$  ( $\Omega_e$  being the equatorial electron gyrofrequency). An important open question then is whether pitch angle scattering retains its diffusive character for several bounce periods. As we will show, the whistler instability (for sufficiently large temperature anisotropy) saturates within few hundreds electron gyroperiods, and the local distribution reaches a quasi-stationary equilibrium, by the time the instability saturates.

## 2. Methodology

We present one-dimensional Particle-in-Cell simulations performed with the implicit moment-method code PARSEK2D [*Markidis et al.*, 2009, 2010]. We are concerned here with a typical situation in the radiation belt,

where whistler waves can be excited by a tenuous population of hot anisotropic electrons. Since we are concerned with timescales much shorter than the bounce period, we are justified in using an homogeneous background magnetic field (i.e. neglecting its dipolar nature)  $B_0 = 4 \cdot 10^{-7} T$ , corresponding approximately to the Earth's equatorial value at  $L \sim 4.3$ . The field is aligned with the box. The electron population has a density of  $15 \text{ cm}^{-3}$ , and it is composed for 98.5% by a cold isotropic Maxwellian (1 eV), and for 1.5% by an anisotropic relativistic bi-Maxwellian distribution  $f(v_{\parallel}, v_{\perp}) \propto \exp[-\alpha_{\perp} \gamma - (\alpha_{\parallel} - \alpha_{\perp}) \gamma_{\parallel}]$  (with  $\gamma = (1 - v^2/c^2)^{-1/2}$ ,  $\gamma_{\parallel} = (1 - v_{\parallel}^2/c^2)^{-1/2}$ ,  $c$  the speed of light, and parallel and perpendicular refer to the background magnetic field) [*Naito*, 2013; *Davidson and Yoon*, 1989]. We choose  $\alpha_{\parallel} = 25$ , and  $\alpha_{\perp} = 4$ . The hot population velocity distribution function has standard deviations  $\sqrt{\langle v_{\parallel}^2 \rangle} = 0.175$ , and  $\sqrt{\langle v_{\perp}^2 \rangle} = 0.325$  (normalized to speed of light) corresponding to nominal temperatures of 8 KeV and 30 KeV, respectively. Thus, the initial anisotropy of the suprathermal component is  $T_{\perp}/T_{\parallel} = 3.75$ . The box length is  $L = 400c/\Omega_e$ . We use 8,000 grid points and a timestep  $\Delta t \Omega_e = 0.015$ . We note that for these simulations the advantages of using an implicit PIC code have not been fully exploited. Namely, the implicit scheme allows to relax the stability constraint (Courant-Friedrichs-Lewy condition) related to the choice of grid size and time step. Such potentiality will be explored in the future for two- and three-dimensional simulations, where the first-principle simulation of a large domain in the radiation belt could become feasible with the implicit PIC.

Temperature anisotropy instabilities have a 'self-destructing' character, in the sense that the generated electromagnetic fluctuations reduce the anisotropy that drives the instability, and therefore a marginal stability condition is usually rapidly reached [*Camporeale and Burgess*, 2008; *Gary et al.*, 2014; *Hellinger et al.*, 2014]. Figure 1 shows the reduction of temperature anisotropy (red line, right axes) and the increasing magnetic field amplitude (black line, left axes). The linear instability saturates around the time  $T \Omega_e = 900$ , and although the anisotropy response to the magnetic field fluctuations is somewhat delayed, the correlation is clear. Indeed, in the early linear phase the instability grows starting from small values, without affecting the electron distribution function until  $\delta B/B_0 \simeq 0.02$  is attained. In Figure 2 we show the spectrogram of the magnetic field (top panel), and the wavepower as function of frequency (bottom panel), calculated over the entire simulation time  $T \Omega_e = 2100$ . The red line in the top panel represents the whistler dispersion relation derived from cold plasma theory, which, despite neglecting the suprathermal component, is still a good approximation. Note that the wavepower is peaked around  $\omega/\Omega_e \sim 0.2$  and it is confined within  $\omega/\Omega_e < 0.6$ . In the bottom panel the black line denotes results from the PIC simulation (and therefore are relatively noisy). The red line is a smoothed fit of the PIC result, and the blue line is the spectrum that will be used for the test-particle calculations. It is a Gaussian centered in  $0.2 \Omega_e$  with width equal to  $0.25 \Omega_e$ . Although it overestimates the wavepower at small frequencies, this is a good approximation of the PIC results in the range  $[0.2 - 0.6] \Omega_e$ .

We emphasize that the PIC approach is first-principle and does not rely on any of the assumptions employed for quasi-linear diffusion codes or test-particle simulations. Moreover, the diagnostics on the particle scattering is readily available. In the simulations presented in this paper we have tracked 8 groups composed of 32,000 particles each, that have been initialized with different pitch angle and energies. Specifically, the initial pitch angles range from 10° to 80°, in intervals of 10°. The initial velocity is chosen such that the particles satisfy (at initial time) the resonant condition

$$\omega - kv \cos \alpha = \Omega_e \sqrt{1 - v^2}. \quad (1)$$

for a chosen value of  $\omega$ . The wavevector  $k$  in Eq. (1) is derived from the cold plasma dispersion relation for whistlers:

$$(kc/\omega)^2 = 1 - \frac{\omega_p^2/\Omega_e^2}{\omega(\omega - \Omega_e)}. \quad (2)$$

For each value of initial pitch angle the tracked particles are initially resonant with  $\omega/\Omega_e = 0.3$ . The initial energy for each group of particles is summarized in Table 1. Note that for particles with  $\alpha < 90^\circ$ , the resonant wave is counter-propagating, that is  $k < 0$ . An important point to make clear is that, although these 8 groups of particles have been tracked for diagnostic purposes, they are in all respects PIC particles, i.e. they contribute to the accumulation of charge and current densities with their proper statistical weight.

### 2.1. Test-particles simulation

Although the main focus of this paper is to comment results derived from PIC simulations, it is still interesting to compare the results against test-particleless simulations. The advantage of test-particleless simulations is that one can specify the electromagnetic field at any spatial location with any desired accuracy. Of course, this is in contrast to gridded methods such as PIC where the field must be interpolated from the grid to the particle locations. On the other hand, test-particleless codes lack the self-consistency and conservation properties of PIC (for instance, particles can be indefinitely accelerated). The interest for test-particles methods in the radiation belt studies stems, on one hand, from their computational speed, and on the other hand from the relationship that exists with quasi-linear diffusion codes. Indeed, it is expected that when the assumptions of quasi-linear theory are satisfied, the Einstein relation between quasi-linear diffusion coefficients and test-particles mean squared displacements  $\langle \Delta\alpha^2 \rangle = 2Dt$  holds. Indeed, *Tao et al.* [2011] have successfully shown that this is the case for small-amplitude parallel propagating whistler, and they have later proved the breakdown of quasi-linear theory for larger amplitudes [*Tao et al.*, 2012]. See also *Liu et al.* [2010] for a discussion on the departure time, that is the time at which  $\langle \Delta\alpha^2 \rangle$  departs from the Einstein relation. In this paper we use the same code described in *Tao et al.* [2011]. The wave spectrum is approximated with 200 modes equally spaced between  $\omega/\Omega_e = 0.009$  and  $\omega/\Omega_e = 0.6$ , each of them weighted according to the Gaussian curve shown in Figure 2 (bottom panel, blue curve). For each run the statistics is performed on 400 particles, advanced in time with a timestep  $\Delta t\Omega_e = 0.01$ .

## 3. Results

The main diagnostics that we study is the mean squared displacements in pitch angle and energy. Such quantities are denoted as  $\langle \Delta\alpha^2 \rangle$ ,  $\langle \Delta E^2 \rangle$ , and  $\langle \Delta E \Delta\alpha \rangle$  (the mixed diffusion term), where  $\Delta\alpha = \alpha - \langle \alpha \rangle$ ,  $\Delta E = E - \langle E \rangle$ , and  $\langle \dots \rangle$  denotes the average over the whole sample. Figure 3 shows the development of  $\langle \Delta\alpha^2 \rangle$  in time for the tracked particles. The different colors are labeled in the legend and correspond to different initial pitch angles. An important feature, and one of the main results of the paper, is that for all angles less than  $70^\circ$ , the pitch angle mean squared displacement  $\langle \Delta\alpha^2 \rangle$  shows two distinct phases: a rapid growth for  $T\Omega_e \lesssim 700$ , and a much slower growth at later times. This behavior is nicely correlated with the linear growth phase shown in Figure 1. Moreover, for the simulation time presented, the dashed line represents an asymptotic value for the resonant particles with initial pitch angle less than  $60^\circ$ . Such dashed line corresponds to the pitch angle variance of an isotropic velocity distribution, but with all the particles bounded to the  $\alpha < 90^\circ$  interval. This is simply calculated by defining the particle distribution function

$f(\alpha) = \sin \alpha$  for  $\alpha \leq 90^\circ$ , and  $f(\alpha) = 0$  for  $\alpha > 90^\circ$ . The mean value of such distribution is equal to 1 rad =  $57.3^\circ$ . The variance in degrees is then calculated as

$$\left(\frac{180^\circ}{\pi}\right)^2 \int_0^{\frac{\pi}{2}} (\alpha - 1)^2 f(\alpha) d\alpha \simeq 465 \text{ (deg}^2\text{)}. \quad (3)$$

In order to understand the behavior shown in Figure 3, and how the asymptotic value of  $465^\circ$  comes about, we look at the evolution of the distribution in pitch angle at different times. Figures 4, 5, 6, and 7 show the histograms of the number of particles at different angles for times  $T\Omega_e = 500, 1000, 1500, 2000$ , for initial pitch angles  $\alpha = 20^\circ, 60^\circ, 70^\circ, 80^\circ$ , respectively. We note that  $T\Omega_2 = 2000$  is still much less than the electron bounce period in the Earth's dipole field, which is estimated at  $14,000 \Omega_e^{-1}$ . A common feature of Figures 4 and 5 (i.e. for initial  $\alpha = 20^\circ$  and  $60^\circ$ ) is that  $90^\circ$  represents a diffusion 'barrier', in the sense that diffusion through  $90^\circ$  is very limited, although not exactly null. The same feature appears for particles with initial pitch angle  $\alpha = 30^\circ, 40^\circ, 50^\circ$  (not shown). This is consistent with standard quasi-linear theory which predicts a very small diffusion coefficient at  $90^\circ$ . This is shown in Figure 8, where the Summers coefficient  $D_{\alpha\alpha}$  at  $90^\circ$  (see Eq. (36) in *Summers* [2005]) is plotted as function of energy for a wave amplitude  $\delta B/B_0 = 0.01$  (note that the coefficient scales linearly with the square of the wave amplitude). For the range of energies and the timescale considered here the pitch angle diffusion coefficient at  $90^\circ$  is essentially null. We note however that, as *Summers et al.* [2007] clarifies, nonlinear effects and phase trapping are not included in the quasi-linear treatment. The bottom-right panels of Figures 4 and 5 also show the analytical isotropic distribution  $f(\alpha)$  discussed previously, as a black line, and they support the argument that since diffusion tends to fill the left half of the distribution, the variance approaches in the time the value of  $465 \text{ (deg}^2\text{)}$ , as shown in Figure 3. Figure 6 has the same format of Figures 4 and 5, but now for initial  $\alpha = 70^\circ$ . The behavior is not very dissimilar, but one can notice a non-negligible fraction of particles diffusing through the  $90^\circ$  barrier. Finally, in Figure 7, we show the histograms for initial pitch angle  $\alpha = 80^\circ$ . The behavior is now qualitatively different, and this was already evident from the mean squared displacement shown in Figure 3. There is no sign of a diffusion barrier at  $90^\circ$ , and at the final stage the distribution is almost symmetrical around  $90^\circ$ . The obtained results are reminiscent of the  $90^\circ$  scattering problem found by quasi-linear theory for the pitch angle diffusion of cosmic rays [e.g., *Goldstein*, 1976; *Qin and Shalchi*, 2014] (and many others). Quasi-linear theory can be seen as a first order perturbation theory where the actual particle trajectories are replaced by trajectories in the unperturbed field; this approach however does not allow to correctly describe pitch angle diffusion close to  $90^\circ$ . The development of a nonlinear theory [*Goldstein*, 1976] shows that pitch angle diffusion is indeed very small, but not null, for  $\alpha = 90^\circ$  and  $\delta B/B_0 = 0.05\text{--}0.1$ , while for  $\delta B/B_0 \simeq 0.3$  the pitch angle scattering rate at  $\alpha = 90^\circ$  is comparable to that at  $\alpha = 60^\circ$  (see Figures 1–4 in *Goldstein* [1976]). Recently, the scaling of the pitch angle diffusion coefficient with  $\delta B/B_0$  and with the cosmic ray energy was considered by *Qin and Shalchi* [2014] using both a second order theory and test particle simulations, and they confirmed the smallness of  $D_{\alpha\alpha}$  for small to moderate levels of  $\delta B/B_0$ . Therefore, we can also interpret our results in terms of the nonlinear theories, considering that from Figure 1 for  $\Omega_e t > 900$  we have  $\delta B/B_0 \simeq 0.06\text{--}0.07$ , corresponding to the range where *Goldstein* [1976] found very small scattering. For completeness, we show in Figures 9 and 10 the energy

mean squared displacement  $\langle \Delta E^2 \rangle$ , and the mixed term  $\langle \Delta E \Delta \alpha \rangle$ , respectively. The role of the mixed diffusion coefficient has been recently discussed at length in the literature (see, e.g., *Subbotin et al.* [2010]; *Zheng et al.* [2011]), and Figure 10 confirms that its magnitude is comparable to  $\langle \Delta \alpha^2 \rangle$  and  $\langle \Delta E^2 \rangle$ .

To conclude this section we present in Figure 11 and 13 a comparison between PIC and test-particles simulations. We interpret test-particles results as representative of the quasi-linear paradigm employed in radiation belt simulations. The aim of such comparison is to show that the fact that the calculation of diffusion coefficients does not take in account the growth rate of a wave due to an ongoing kinetic instability, can lead to an erroneous prediction of pitch angle scattering. In comparing PIC and test-particles simulations, it is important to remind that in the latter the field amplitude is constant, and thus one would not expect a good agreement for long times. Hence the test-particles simulations are run for 300 gyroperiods only (the disagreement with PIC, however, is evident since initial times). Figure 11 shows as a black line the pitch angle mean squared displacement  $\langle \Delta \alpha^2 \rangle$  for initial  $\alpha = 20^\circ$  (same plot as in Figure 3). We have superposed, with red lines, the results of test-particles runs, considering the instantaneous (increasing) value of magnetic field perturbation  $\delta B/B_0$ , at different times. For clarity, the red lines (test-particles results) starting points are vertically offset so that they are made coincide with the PIC result (black line). The six red lines are for values  $\delta B/B_0 = 0.01, 0.02, \dots, 0.06$ . As expected, larger values of  $\delta B/B_0$  result in a more rapid growth of the mean squared displacement  $\langle \Delta \alpha^2 \rangle$ , for test-particles. Indeed, if we assume quasi-linear theory to hold, the diffusion coefficient can be calculated as the time derivative of  $\langle \Delta \alpha^2 \rangle$ , i.e. the slope of the red lines in Figure 11. As we said, such diffusion coefficient scales quadratically with  $\delta B/B_0$  (see Eq. 36 in *Summers* [2005]). A very clear and striking result from Figure 11 is that the test-particles prediction underestimates the pitch angle scattering in the linear growth phase ( $T\Omega_e \lesssim 600$ ), and largely overestimates the scattering in the saturation regime ( $T\Omega_e \gtrsim 700$ ). The main reason why test-particles are unable to correctly predict the evolution of  $\langle \Delta \alpha^2 \rangle$  in Figure 11 is because the time derivative of  $\langle \Delta \alpha^2 \rangle$  (i.e. the effective diffusion coefficient, in the quasi-linear context) does not monotonically increase with  $\delta B/B_0$ . Figure 12 shows the time derivative of  $\langle \Delta \alpha^2 \rangle$  as function of the instantaneous  $\delta B/B_0$ , calculated from PIC particles. Evidently, there is not a persistent monotonic correlation between the two quantities. It is also possible that for  $\delta B/B_0 \geq 0.05$  phase trapping in the whistler waves occurs, as recently considered by *Shklyar and Zimbardo* [2014]. Under such premises, it is no surprise that test-particles and the resonant limit of quasi-linear theory are unusable. The same discrepancy occurs for all particles with initial  $\alpha \lesssim 60^\circ$ , that is particles for which the mean squared displacement in pitch angle 'saturates' in time (Figure 3). We have already commented on the fact that such saturation occurs as the result that the particles see a strong diffusion barrier at  $90^\circ$ , and they effectively reach a stationary (or quasi-stationary) distribution. Of course the diffusion coefficient is very small but not exactly null at  $90^\circ$ , and after a sufficiently long time they will diffuse to  $\alpha > 90^\circ$ . Such long time evolution is not of interest for radiation belts, since electron precipitation into the loss cone will modify  $f(\alpha)$  much earlier. In different contexts, it is important to point out that when electrons are unable to overcome the  $90^\circ$  barrier, their parallel velocity has a constant sign. This fact gives rise to very long displacements along the magnetic field, which are eventually reversed when  $\alpha > 90^\circ$ . When considering spatial diffusion, these long displacements can be at the origin of superdiffusive transport in the parallel direction, as observed in the solar wind [e.g., *Perri and Zimbardo*, 2007] and as discussed by *Perrone et al.* [2013]; *Zimbardo and Perri* [2013]. Indeed,

the  $90^\circ$  barrier for pitch angle scattering creates a persistent statistical process for  $v_{\parallel}$ . This also highlights the need to study pitch angle scattering in the nonlinear, self-consistent regime.

As expected, a different phenomenology occurs for particles that do not saturate, i.e. for initial pitch angle  $\alpha > 60^\circ$ . For instance, the case with initial  $\alpha = 70^\circ$  is plotted in Figure 13. Here, there seems to be a much better agreement between PIC and test-particles. However, it is important to notice that, for times  $T \lesssim 600$  (i.e. linear growth phase), the test-particles still underestimate the pitch angle scattering. The better agreement from time  $T \gtrsim 600$  with respect to the  $\alpha = 20^\circ$  case (Figure 11) is due to the fact that the magnetic field perturbation becomes close to saturation and hence the (instantaneous) diffusion coefficient does not vary. Furthermore, the  $70^\circ$  particles are not subject to the  $90^\circ$  diffusion barrier, and hence they continue diffusing. Their mean squared displacement  $\langle \Delta \alpha^2 \rangle$  does not saturate abruptly as for the  $\alpha = 20^\circ$  case and hence there is a more prolonged time for which PIC and test-particles are in an approximate agreement. In conclusions, the results for resonant particles (i.e., particles whose initial pitch angle and energy satisfy the resonance condition with a wave with frequency  $\omega/\Omega_e = 0.3$ ) can be summarized as follows. A distinguishing feature that marks a qualitatively different dynamics is whether the particles diffuse or not through the  $90^\circ$  barrier (within a short timescale). Particles that do not diffuse through the barrier tend to reach a quasi-stationary isotropic distribution that fills half domain in pitch angle. The evolution of their mean squared displacement is strongly correlated with the linear growth and non-linear saturation of the magnetic field perturbation. Quasi-linear or test-particles predictions does not seem to be applicable to such particles, on the basis that the ongoing wave growth makes the instantaneous diffusion coefficient (if one still wants to interpret the dynamics as diffusive) not monotonically correlated with the wave amplitude. In other words, the time dependency of the wave power and the pitch angle scattering nonlinearly regulate each other. The crucial point is that most of the scattering occurs during the linear phase, contrary to the assumptions of the resonant limit of quasi-linear theory previously discussed.

## 4. Conclusions

We have presented PIC and test-particles simulations of resonant wave-particle interactions between lower band whistler modes and anisotropic electrons, with parameters that realistically mimic the injection of energetic particles at equatorial latitude, for  $L \sim 4.3$ . In PIC simulations, the whistler waves are generated self-consistently, and as a consequence the initial particle anisotropy is reduced towards a marginal stable configuration. The focus has been on analyzing the statistics of PIC particles, in particular their mean squared displacement in energy and pitch angle, both during the linear growth phase, and in the nonlinear saturation regime. This approach differs from the quasi-linear theory and test-particles simulations, which usually (although not by construction) assume a constant (non-growing) wave field amplitude. We have used test-particles simulations to compare and appreciate the deficiencies of the (resonant limit of the) quasi-linear treatment. The main results of the paper can be summarized as follows:

- The evolution of the mean squared displacements is very well correlated with the linear wave growth and its subsequent saturation. Enhanced diffusion is observed during the linear growth phase, in a much larger measure than after saturation;

- For most angles, the distribution in pitch angle saturates and very rapidly reaches a quasi-stationary equilibrium, in a few hundreds gyroperiods, that is in a fraction of the bounce period;

- Although the  $90^\circ$  barrier is very effective for most energy/angles, a non-negligible fraction of particles can actually diffuse through the barrier; whether particles diffuse or not through  $90^\circ$  determine the dynamics and the saturation (or lack of it) of the mean squared displacement (within the simulation time: because the domain is bounded all particles will eventually saturate in pitch angle);

- The disagreement with quasi-linear theory and test-particles simulations can be attributed both on neglecting the rapid growth rate of the linear wave, and on the lack of  $90^\circ$  diffusion.

In conclusion, this paper emphasizes the importance of a self-consistent treatment of pitch angle and energy diffusion during the growth phase of whistlers. In a realistic scenario one can envision that the effect of several injection of anisotropic energetic particles in a short time can result in an overall enhanced diffusion that can cumulatively affect the dynamics of particle loss, and thus should be taken in account for realistic estimates. The inclusion of nonlinear (or higher-order) effect in the calculation of wave-particle interactions is recently becoming a topic of interest, following the discovery of very large amplitude whistler-mode waves in Earth's radiation belts by Cattell *et al.* [2008] (see also [Kersten *et al.*, 2011; Mozer *et al.*, 2013]).

The results discussed in this paper might also be relevant to other context. For instance, the generation of suprathermal electrons by resonant wave-particle interactions has been discussed at length for the solar wind [e.g. Pierrard *et al.*, 1999; Vocks and Mann, 2003; Vocks *et al.*, 2005; Saito and Gary, 2007]. On the other hand, it is well-known that magnetized plasma turbulence exhibits features typical of super or sub-diffusive processes [Zimbardo and Perri, 2013; Perrone *et al.*, 2013]. Also, the role of whistler wave is been currently investigated in solar wind turbulence [Gary and Smith, 2009; Camporeale and Burgess, 2011; Lacombe *et al.*, 2014]. Finally, as already mentioned, wave-particle interactions has been a long-time topic well studied in connection to cosmic-ray acceleration [Schlickeiser *et al.*, 2010].

Although this paper has focused on one-dimensional simulations, the implicit PIC algorithm will allow in the near future to tackle fully consistent simulations of wave-particle interaction on multi-dimensions, possibly including multi-scale dynamics.

**Acknowledgments.** We thank X. Tao for sharing his test-particles code, and for insightful comments. EC wishes to acknowledge J. Bortnik and G. Reeves for useful discussions. The output data from our simulations is available upon request to the corresponding author (e.camporeale@cwi.nl)

## References

- Albert, J., and Y. Shprits (2009), Estimates of lifetimes against pitch angle diffusion, *Journal of Atmospheric and Solar-Terrestrial Physics*, 71(16), 1647–1652.
- Bickel, T. (2007), A note on confined diffusion, *Physica A: Statistical Mechanics and its Applications*, 377(1), 24–32.
- Camporeale, E., and D. Burgess (2008), Electron firehose instability: Kinetic linear theory and two-dimensional particle-in-cell simulations, *Journal of Geophysical Research: Space Physics* (1978–2012), 113(A7).
- Camporeale, E., and D. Burgess (2011), The dissipation of solar wind turbulent fluctuations at electron scales, *The Astrophysical Journal*, 730(2), 114.
- Cattell, C., J. Wygant, K. Goetz, K. Kersten, P. Kellogg, T. Von Rosenvinge, S. Bale, I. Roth, M. Temerin, M. Hudson, et al. (2008), Discovery of very large amplitude whistler-mode waves in earth's radiation belts, *Geophysical Research Letters*, 35(1).
- Davidson, R. C., and P. H. Yoon (1989), Nonlinear bound on unstable field energy in relativistic electron beams and plasmas, *Physics of Fluids B: Plasma Physics (1989-1993)*, 1(1), 195–203.
- Fu, X., M. M. Cowee, R. H. Friedel, H. O. Funsten, S. P. Gary, G. B. Hospodarsky, C. Kletzing, W. Kurth, B. A. Larsen, K. Liu, et al. (2014), Whistler anisotropy instabilities as the source of banded chorus: Van allen probes observations and particle-in-cell simulations, *Journal of Geophysical Research: Space Physics*, 119(10), 8288–8298.
- Gary, S. P., and C. W. Smith (2009), Short-wavelength turbulence in the solar wind: Linear theory of whistler and kinetic alfvén fluctuations, *Journal of Geophysical Research: Space Physics* (1978–2012), 114(A12).
- Gary, S. P., R. S. Hughes, J. Wang, and O. Chang (2014), Whistler anisotropy instability: Spectral transfer in a three-dimensional particle-in-cell simulation, *Journal of Geophysical Research: Space Physics*, 119(3), 1429–1434.
- Glauert, S. A., and R. B. Horne (2005), Calculation of pitch angle and energy diffusion coefficients with the PADIE code, *Journal of Geophysical Research (Space Physics)*, 110(A9), A04206, doi:10.1029/2004JA010851.
- Goldstein, M. L. (1976), A nonlinear theory of cosmic-ray pitch-angle diffusion in homogeneous magnetostatic turbulence, *The Astrophysical Journal*, 204, 900–919.
- Hellinger, P., P. M. Trávníček, V. K. Decyk, and D. Schriver (2014), Oblique electron fire hose instability: Particle-in-cell simulations, *Journal of Geophysical Research: Space Physics*, 119(1), 59–68.
- Hikishima, M., S. Yagitani, Y. Omura, and I. Nagano (2009), Full particle simulation of whistler-mode rising chorus emissions in the magnetosphere, *Journal of Geophysical Research: Space Physics* (1978–2012), 114(A1).
- Jokipii, J. (1966), Cosmic-ray propagation. i. charged particles in a random magnetic field, *The Astrophysical Journal*, 146, 480.
- Jordanova, V. K., R. M. Thorne, W. Li, and Y. Miyoshi (2010), Excitation of whistler mode chorus from global ring current simulations, *Journal of Geophysical Research (Space Physics)*, 115, A00F10, doi:10.1029/2009JA014810.
- Katoh, Y., and Y. Omura (2007a), Computer simulation of chorus wave generation in the earth's inner magnetosphere, *Geophysical research letters*, 34(3).
- Katoh, Y., and Y. Omura (2007b), Relativistic particle acceleration in the process of whistler-mode chorus wave generation, *Geophysical research letters*, 34(13).
- Kennel, C., and F. Engelmann (1966), Velocity space diffusion from weak plasma turbulence in a magnetic field, *Physics of Fluids*, 9(12), 2377.
- Kersten, K., C. Cattell, A. Breneman, K. Goetz, P. Kellogg, J. Wygant, L. Wilson, J. Blake, M. Looper, and I. Roth (2011), Observation of relativistic electron microbursts in conjunction with intense radiation belt whistler-mode waves, *Geophysical Research Letters*, 38(8).
- Lacombe, C., O. Alexandrova, L. Matteini, O. Santolik, N. Cornilleau-Wehrin, A. Mangeney, Y. de Conchy, and M. Maksimovic (2014), Whistler mode waves and the electron heat flux in the solar wind: Cluster observations, *The Astrophysical Journal*, 796(1), 5.
- Liu, K., D. S. Lemons, D. Winske, and S. P. Gary (2010), Relativistic electron scattering by electromagnetic ion cyclotron fluctuations: Test particle simulations, *Journal of Geophysical Research: Space Physics* (1978–2012), 115(A4).
- Lyons, L. R., and R. M. Thorne (1973), Equilibrium structure of radiation belt electrons, *Journal of Geophysical Research*, 78(13), 2142–2149.
- Markidis, S., E. Camporeale, D. Burgess, G. Lapenta, et al. (2009), Parsek2d: An implicit parallel particle-in-cell code, in *Numerical Modeling of Space Plasma Flows: ASTRONUM-2008*, vol. 406, p. 237.
- Markidis, S., G. Lapenta, et al. (2010), Multi-scale simulations of plasma with ipic3d, *Mathematics and Computers in Simulation*, 80(7), 1509–1519.
- Metzler, R., and J. Klafter (2000), Boundary value problems for fractional diffusion equations, *Physica A: Statistical Mechanics and its Applications*, 278(1), 107–125.

- Mourenas, D., and J.-F. Ripoll (2012), Analytical estimates of quasi-linear diffusion coefficients and electron lifetimes in the inner radiation belt, *Journal of Geophysical Research (Space Physics)*, *117*, A01204, doi:10.1029/2011JA016985.
- Mozer, F., S. Bale, J. Bonnell, C. Chaston, I. Roth, and J. Wygant (2013), Megavolt parallel potentials arising from double-layer streams in the earths outer radiation belt, *Physical review letters*, *111*(23), 235,002.
- Naito, O. (2013), A model distribution function for relativistic bi-maxwellian with drift, *Physics of Plasmas (1994-present)*, *20*(4), 044,501.
- Omura, Y., Y. Katoh, and D. Summers (2008), Theory and simulation of the generation of whistler-mode chorus, *Journal of Geophysical Research: Space Physics (1978-2012)*, *113*(A4).
- Omura, Y., D. Nunn, and D. Summers (2012), Generation processes of whistler mode chorus emissions: Current status of nonlinear wave growth theory, *Dynamics of the Earth's Radiation Belts and Inner Magnetosphere*, pp. 243–254.
- Perri, S., and G. Zimbardo (2007), Evidence of superdiffusive transport of electrons accelerated at interplanetary shocks, *The Astrophysical Journal Letters*, *671*(2), L177.
- Perrone, D., R. Dendy, I. Furno, R. Sanchez, G. Zimbardo, A. Bovet, A. Fasoli, K. Gustafson, S. Perri, P. Ricci, et al. (2013), Nonclassical transport and particle-field coupling: from laboratory plasmas to the solar wind, *Space Science Review*, doi:10.1007/s11214-013-9966-9.
- Pierrard, V., M. Maksimovic, and J. Lemaire (1999), Electron velocity distribution functions from the solar wind to the corona, *Journal of Geophysical Research: Space Physics (1978-2012)*, *104*(A8), 17,021–17,032.
- Qin, G., and A. Shalchi (2009), Pitch-angle diffusion coefficients of charged particles from computer simulations, *The Astrophysical Journal*, *707*(1), 61.
- Qin, G., and A. Shalchi (2014), Detailed numerical investigation of 90 scattering of energetic particles interacting with magnetic turbulence, *Physics of Plasmas (1994-present)*, *21*(4), 042,906.
- Ragot, B. (2012), Pitch-angle scattering: Resonance versus non-resonance, a basic test of the quasilinear diffusive result, *The Astrophysical Journal*, *744*(1), 75.
- Saito, S., and S. P. Gary (2007), Whistler scattering of suprathermal electrons in the solar wind: Particle-in-cell simulations, *Journal of Geophysical Research: Space Physics (1978-2012)*, *112*(A6).
- Schlickeiser, R., M. Lazar, and M. Vukcevic (2010), The influence of dissipation range power spectra and plasma-wave polarization on cosmic-ray scattering mean free path, *The Astrophysical Journal*, *719*(2), 1497.
- Shalchi, A., and R. Schlickeiser (2005), Evidence for the nonlinear transport of galactic cosmic rays, *The Astrophysical Journal Letters*, *626*(2), L97.
- Shklyar, D., and G. Zimbardo (2014), Particle dynamics in the field of two waves in a magnetoplasma, *Plasma Physics and Controlled Fusion*, *56*(9), 095,002.
- Shprits, Y. Y., N. P. Meredith, and R. M. Thorne (2007), Parameterization of radiation belt electron loss timescales due to interactions with chorus waves, *Geophysical research letters*, *34*(11).
- Subbotin, D., Y. Shprits, and B. Ni (2010), Three-dimensional verb radiation belt simulations including mixed diffusion, *Journal of Geophysical Research: Space Physics (1978-2012)*, *115*(A3).
- Summers, D. (2005), Quasi-linear diffusion coefficients for field-aligned electromagnetic waves with applications to the magnetosphere, *Journal of Geophysical Research (Space Physics)*, *110*(A9), A08213, doi:10.1029/2005JA011159.
- Summers, D., R. M. Thorne, and F. Xiao (1998), Relativistic theory of wave-particle resonant diffusion with application to electron acceleration in the magnetosphere, *Journal of Geophysical Research: Space Physics (1978-2012)*, *103*(A9), 20,487–20,500.
- Summers, D., B. Ni, and N. P. Meredith (2007), Timescales for radiation belt electron acceleration and loss due to resonant wave-particle interactions: 1. Theory, *Journal of Geophysical Research (Space Physics)*, *112*, A04206, doi: 10.1029/2006JA011801.
- Summers, D., B. Ni, and N. P. Meredith (2007), Timescales for radiation belt electron acceleration and loss due to resonant wave-particle interactions: 2. evaluation for vlf chorus, elf hiss, and electromagnetic ion cyclotron waves, *Journal of Geophysical Research: Space Physics (1978-2012)*, *112*(A4).
- Summers, D., R. Tang, and Y. Omura (2012), Linear and nonlinear growth of magnetospheric whistler mode waves, *Dynamics of the Earth's Radiation Belts and Inner Magnetosphere*, pp. 265–280.
- Tao, X. (2014), A numerical study of chorus generation and the related variation of wave intensity using the dawn code, *Journal of Geophysical Research: Space Physics*.
- Tao, X., J. Bortnik, J. Albert, K. Liu, and R. Thorne (2011), Comparison of quasilinear diffusion coefficients for parallel propagating whistler mode waves with test particle simulations, *Geophysical Research Letters*, *38*(6).
- Tao, X., J. Bortnik, J. M. Albert, and R. M. Thorne (2012), Comparison of bounce-averaged quasi-linear diffusion coefficients for parallel propagating whistler mode waves with test particle simulations, *Journal of Geophysical Research: Space Physics (1978-2012)*, *117*(A10).
- Tautz, R., A. Shalchi, and R. Schlickeiser (2008), Solving the 90 scattering problem in isotropic turbulence, *The Astrophysical Journal Letters*, *685*(2), L165.
- Thorne, R. M. (2010), Radiation belt dynamics: The importance of wave-particle interactions, *Geophysical Research Letters*, *37*(22).
- Vocks, C., and G. Mann (2003), Generation of suprathermal electrons by resonant wave-particle interaction in the solar corona and wind, *The Astrophysical Journal*, *593*(2), 1134.
- Vocks, C., C. Salem, R. Lin, and G. Mann (2005), Electron halo and strahl formation in the solar wind by resonant interaction with whistler waves, *The Astrophysical Journal*, *627*(1), 540.
- Zheng, Q., M.-C. Fok, J. Albert, R. B. Horne, and N. P. Meredith (2011), Effects of energy and pitch angle mixed diffusion on radiation belt electrons, *Journal of Atmospheric and Solar-Terrestrial Physics*, *73*(7), 785–795.
- Zimbardo, G., and S. Perri (2013), From lévy walks to superdiffusive shock acceleration, *The Astrophysical Journal*, *778*(1), 35.

---

Corresponding author: E. Camporeale (e.camporeale@cwi.nl)

**Table 1.** Initial energy in KeV for the tracked resonant groups of particles

| Initial pitch angle | Energy |
|---------------------|--------|
| $\alpha = 10^\circ$ | 28.5   |
| $\alpha = 20^\circ$ | 31.0   |
| $\alpha = 30^\circ$ | 36.0   |
| $\alpha = 40^\circ$ | 44.9   |
| $\alpha = 50^\circ$ | 61.1   |
| $\alpha = 60^\circ$ | 92.8   |
| $\alpha = 70^\circ$ | 163    |
| $\alpha = 80^\circ$ | 358    |

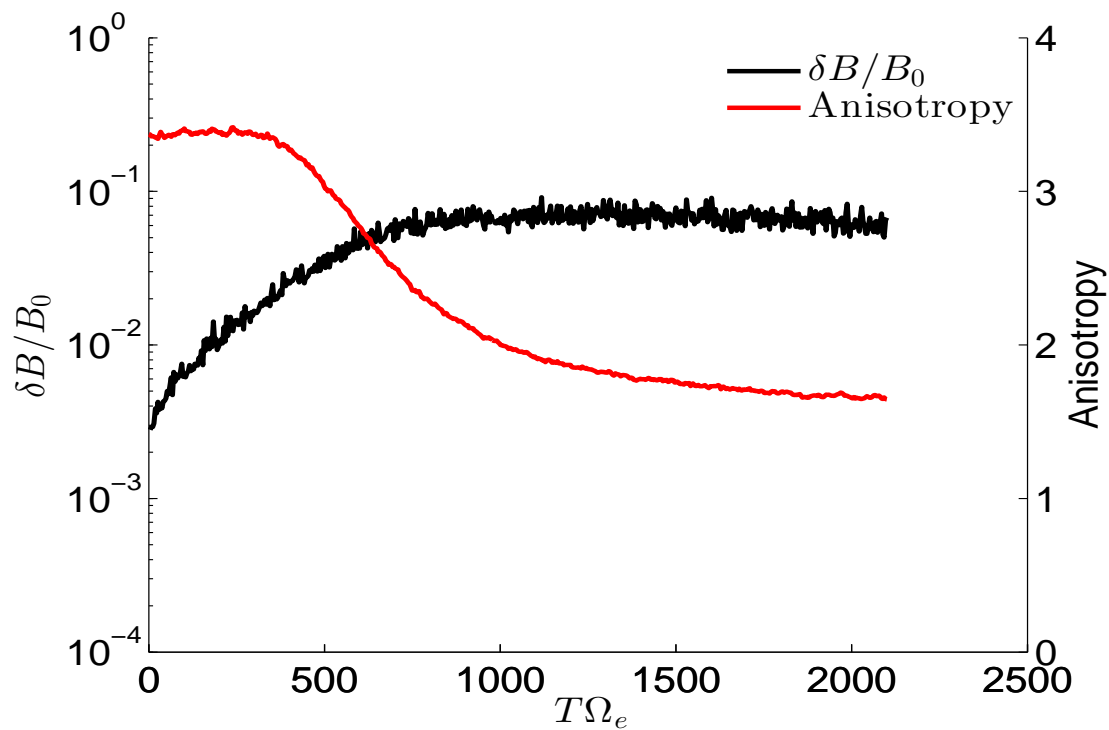


**Figure 1.** Magnetic field relative amplitude  $\delta B/B_0$  (black line, left axes in logarithmic scale), and anisotropy  $T_{\perp}/T_{\parallel}$  (red line, right axes in linear scale) as a function of time  $T\Omega_e$

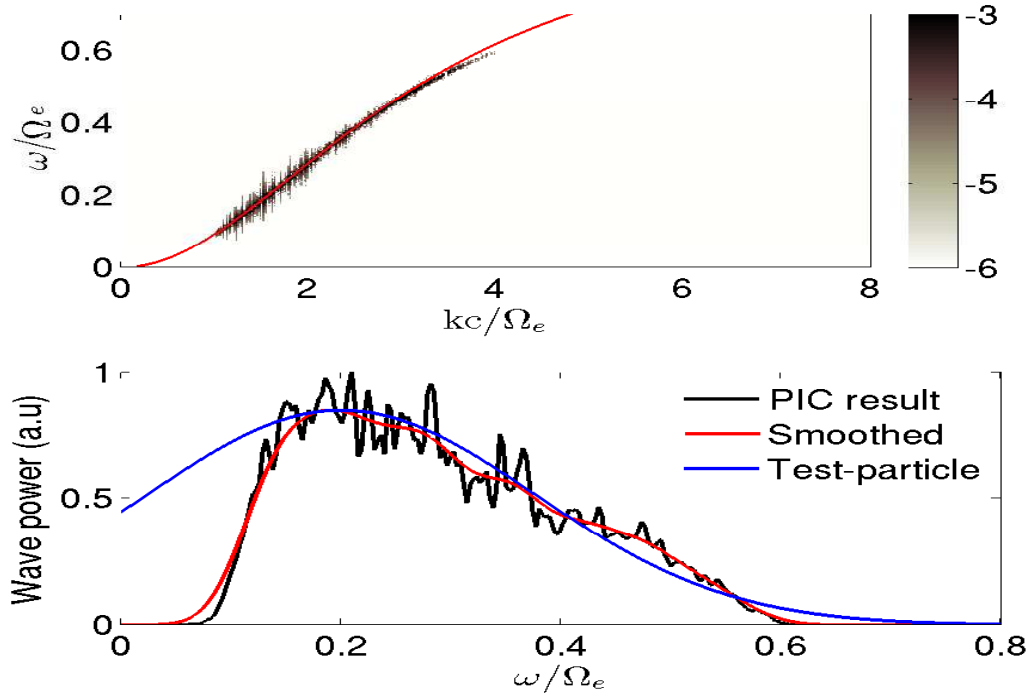


**Figure 2.** Top: spectrogram of magnetic fluctuations in logarithmic scale (frequency vs wavevector). The red line shows the dispersion relation from cold plasma theory. Bottom: wavepower as function of frequency. Black, red, and blue line represent the result from PIC simulations, a smoothed fit, and the Gaussian spectrum used for test-particles simulations.

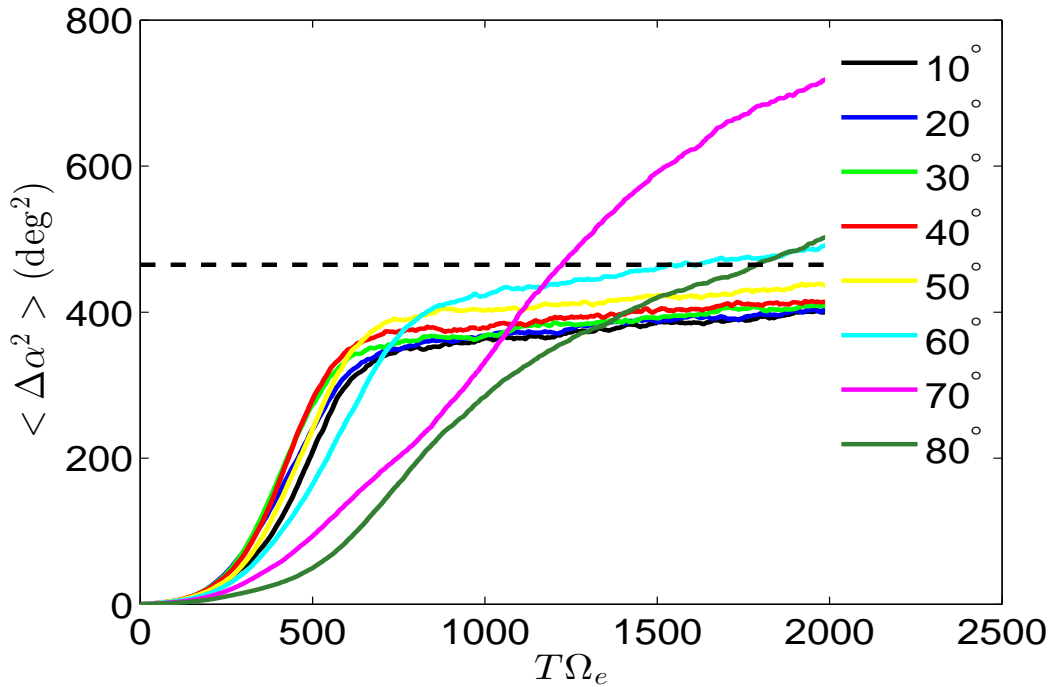


**Figure 3.** Evolution of the pitch angle mean squared displacement  $\langle \Delta\alpha^2 \rangle$  in time. Different colors are for different initial pitch angle. The black dashed line denotes the saturation value  $465 \text{ deg}^2$  (see text for discussion).

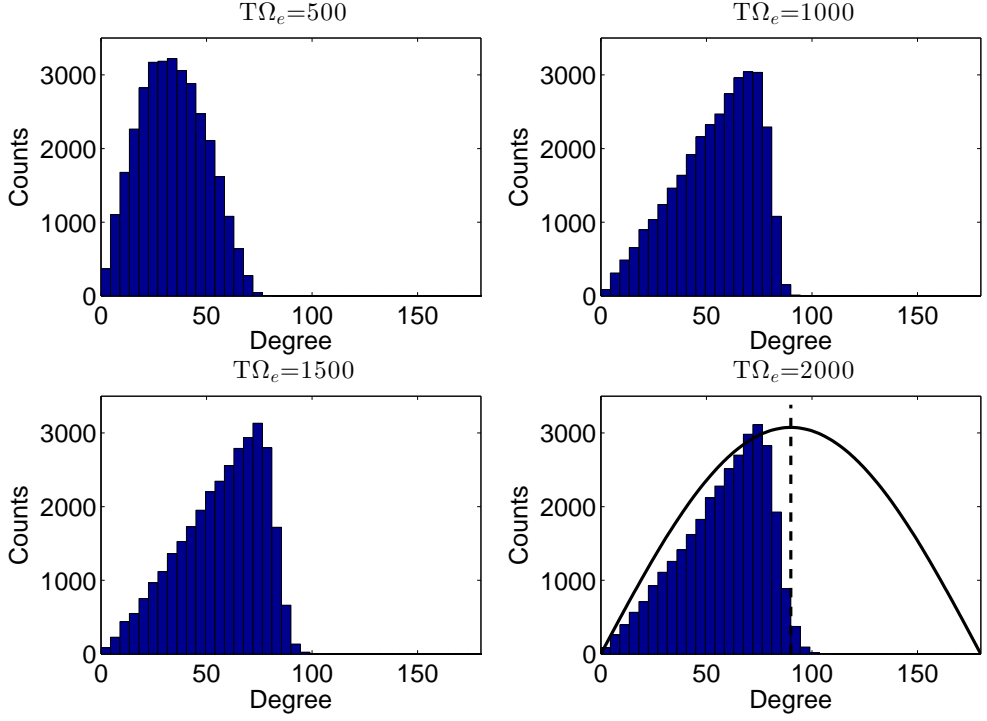


**Figure 4.** Histograms of pitch angle distribution for tracked particles with initial pitch angle  $\alpha = 20^\circ$ , at times  $T\Omega_e = 500, 1000, 1500, 2000$ . The solid line in the right-bottom panel represents the isotropic distribution  $f(\alpha) = \sin \alpha$ , and the vertical dashed line denotes  $\alpha = 90^\circ$ .

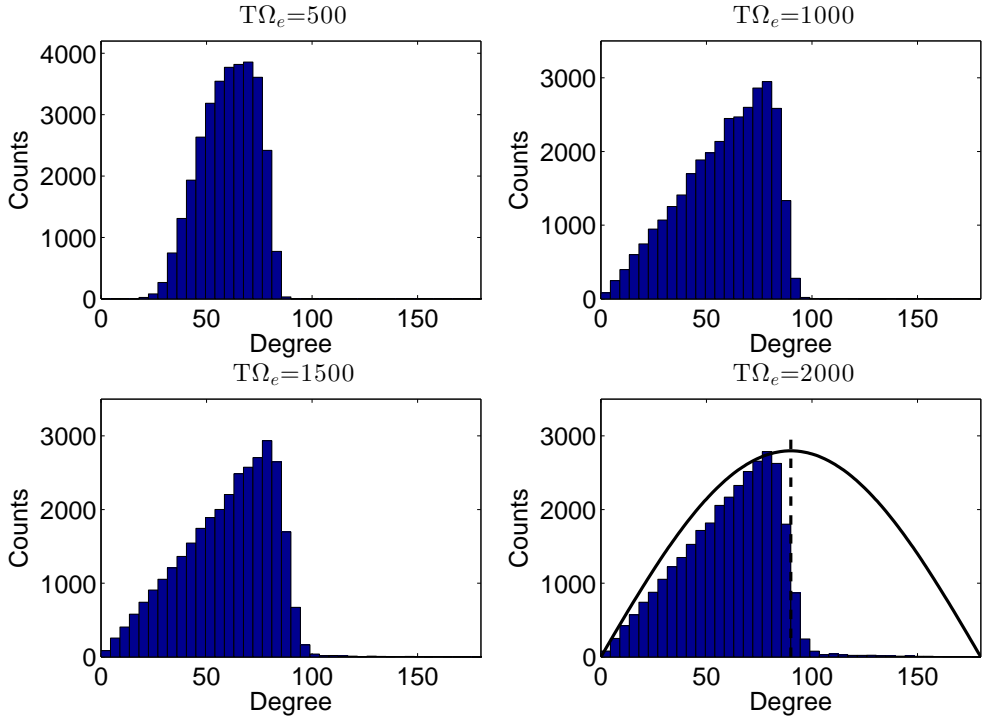


**Figure 5.** Histograms of pitch angle distribution for tracked particles with initial pitch angle  $\alpha = 60^\circ$ , at times  $T\Omega_e = 500, 1000, 1500, 2000$ . The solid line in the right-bottom panel represents the isotropic distribution  $f(\alpha) = \sin \alpha$ , and the vertical dashed line denotes  $\alpha = 90^\circ$ .

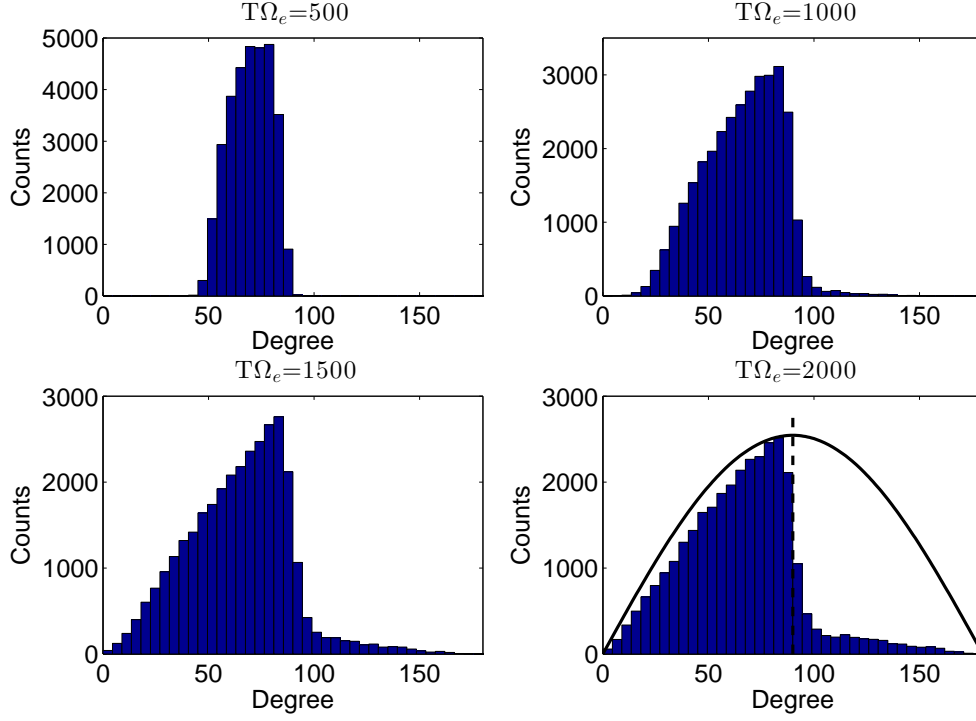


**Figure 6.** Histograms of pitch angle distribution for tracked particles with initial pitch angle  $\alpha = 70^\circ$ , at times  $T\Omega_e = 500, 1000, 1500, 2000$ . The solid line in the right-bottom panel represents the isotropic distribution  $f(\alpha) = \sin \alpha$ , and the vertical dashed line denotes  $\alpha = 90^\circ$ .

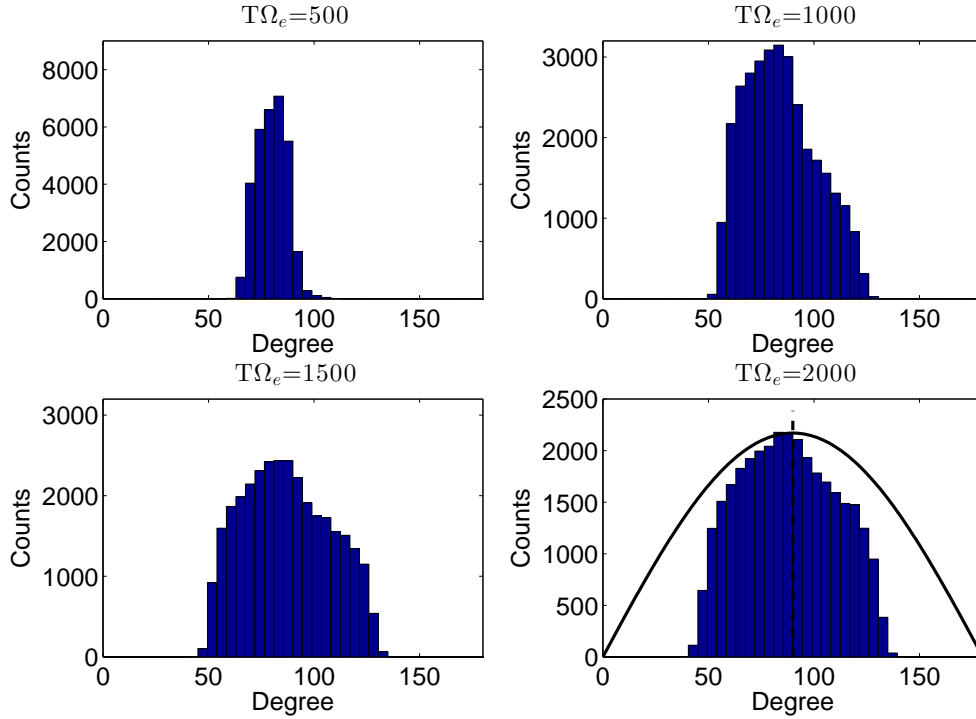


**Figure 7.** Histograms of pitch angle distribution for tracked particles with initial pitch angle  $\alpha = 80^\circ$ , at times  $T\Omega_e = 500, 1000, 1500, 2000$ . The solid line in the right-bottom panel represents the isotropic distribution  $f(\alpha) = \sin \alpha$ , and the vertical dashed line denotes  $\alpha = 90^\circ$ .

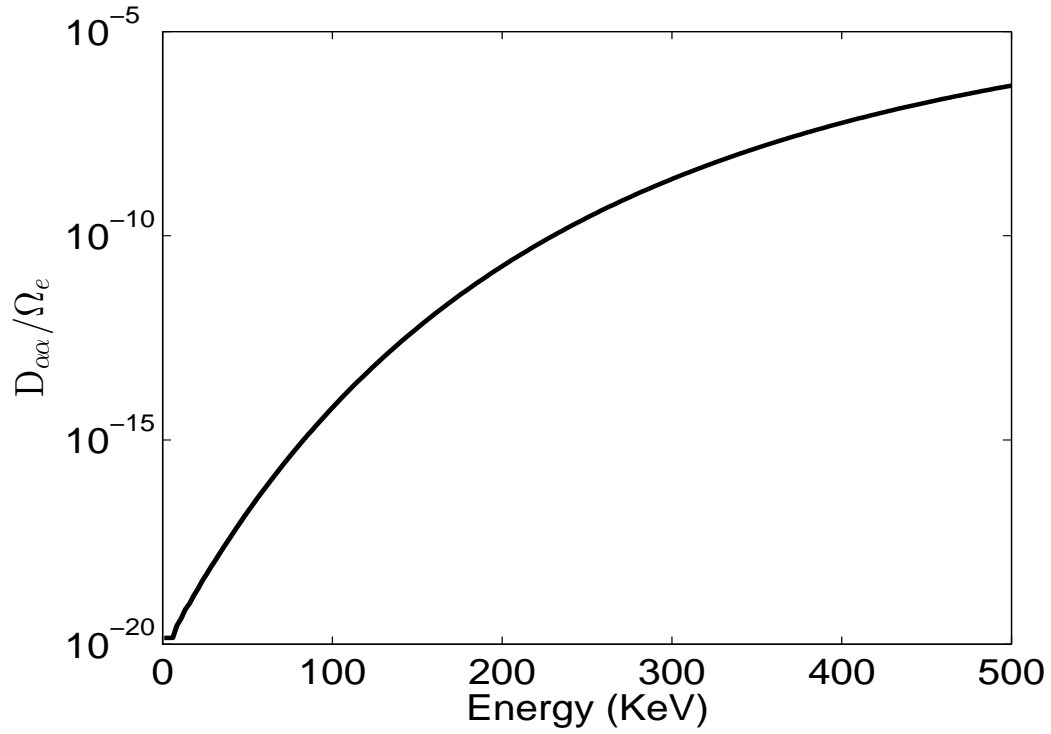


Figure 8. Diffusion coefficient  $D_{\alpha\alpha}$  calculated for  $\alpha = 90^\circ$ , for  $\delta B/B_0 = 0.01$ , as function of energy (in KeV).

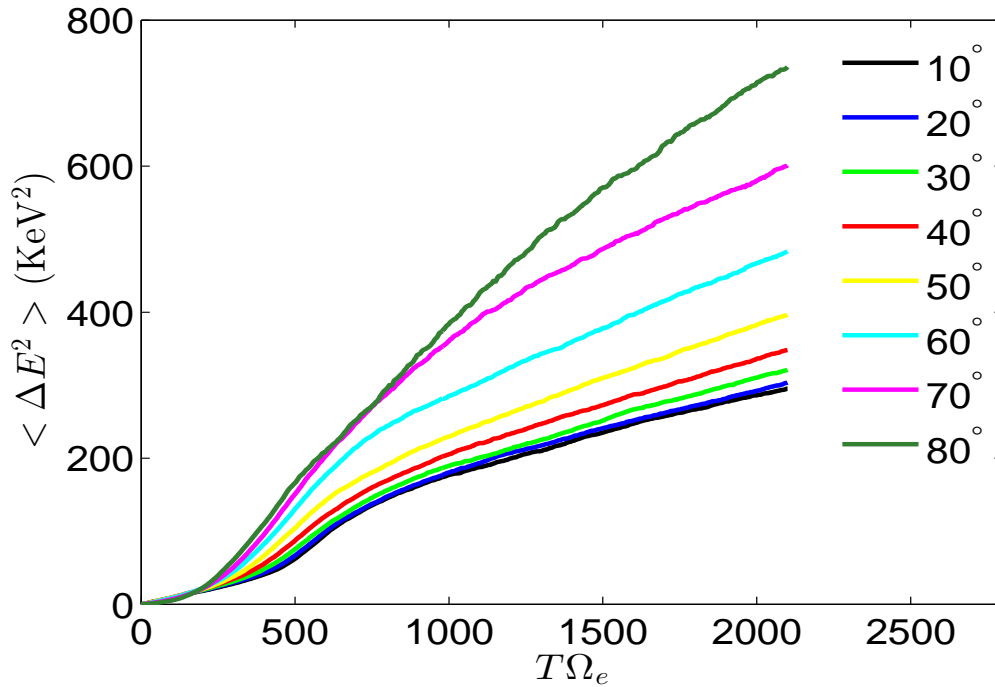
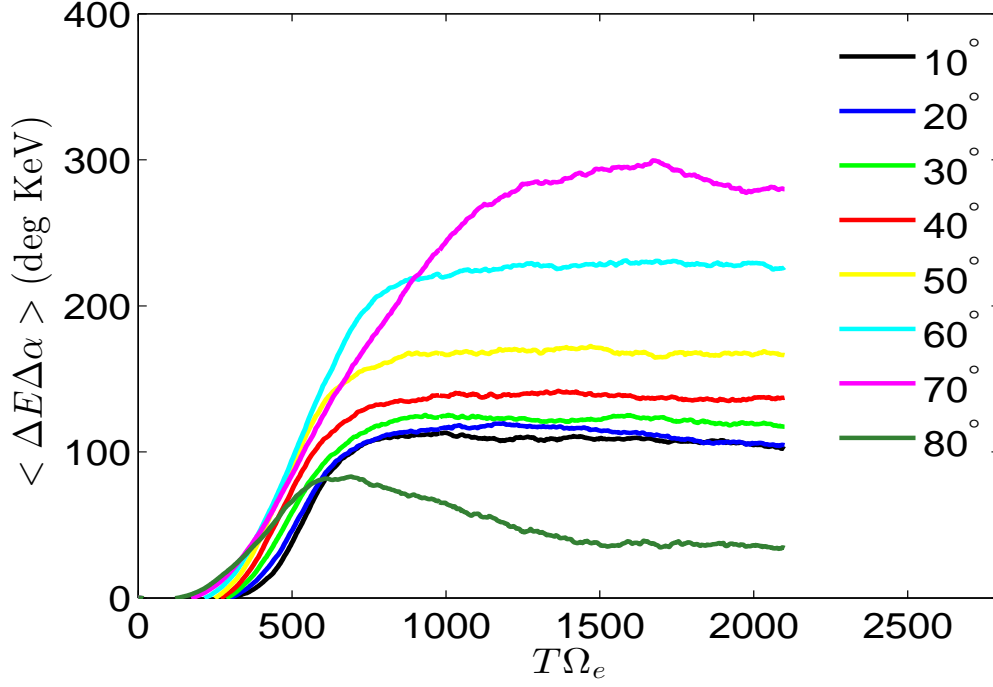
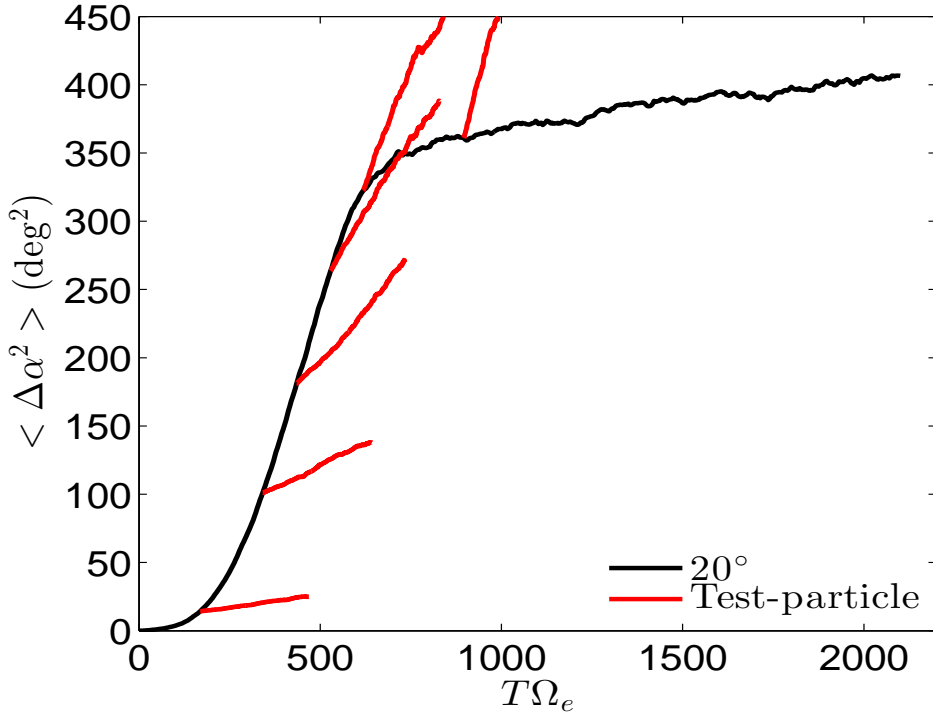


Figure 9. Evolution of the energy mean squared displacement  $\langle \Delta E^2 \rangle$  in time. Different colors are for different initial pitch angle.



**Figure 10.** Evolution of the mean squared displacement  $\langle \Delta E \Delta \alpha \rangle$  (i.e. the mixed diffusion term) in time. Different colors are for different initial pitch angle.



**Figure 11.** Comparison of PIC results with test-particles simulations. The black line denotes  $\langle \Delta \alpha^2 \rangle$  for initial pitch angle  $\alpha = 20^\circ$  (same as in Figure 3). The red lines denotes the results from test-particles. Different red lines are for different simulations initialized with increasing values of  $\delta B/B_0$ . The lines are then superposed starting from the time at which the same value of  $\delta B/B_0$  is reached in the PIC simulation.

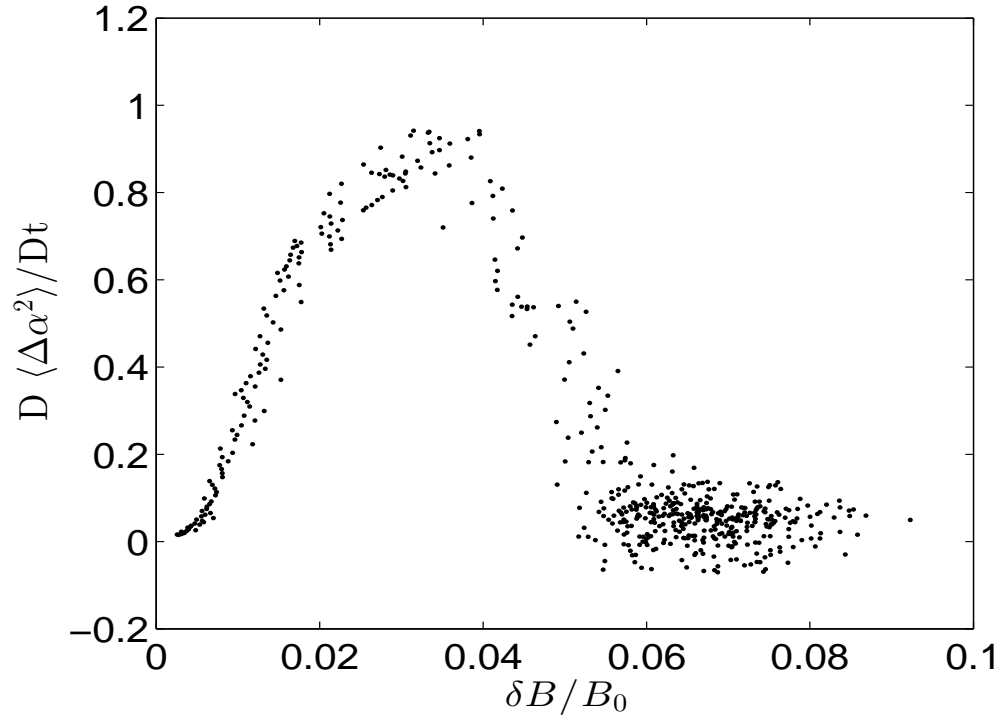


**Figure 12.** Time derivative of  $\langle \Delta\alpha^2 \rangle$  for the  $\alpha = 20^\circ$  case, as function of the instantaneous value of  $\delta B/B_0$ .

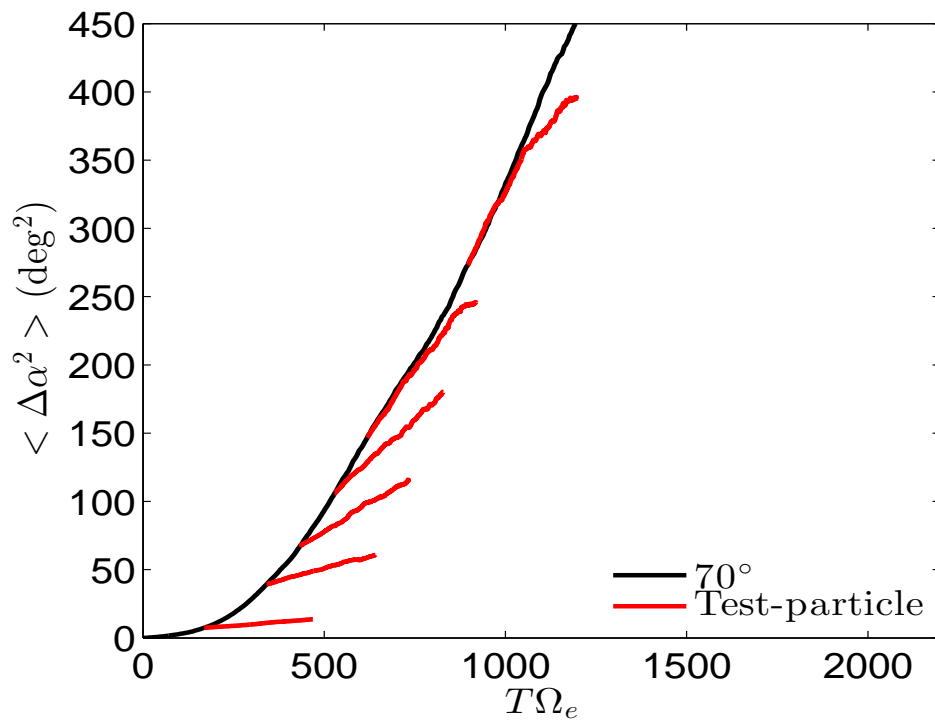


**Figure 13.** Same as figure 11, but for initial  $\alpha = 70^\circ$ .